Multi-targeted multi-color *in vivo* optical imaging in a model of disseminated peritoneal ovarian cancer

Nobuyuki Kosaka
Mikako Ogawa
Michelle R. Longmire
Peter L. Choyke
Hisataka Kobayashi
National Institutes of Health
National Cancer Institute
Center for Cancer Research
Molecular Imaging Program
10 Center Drive
Bethesda, Maryland 20892-1088

Abstract. Commonly used in flow cytometry, multiplexed optical probes can diagnose multiple types of cell surface marker, potentially leading to improved diagnosis accuracy *in vivo*. Herein, we demonstrate the targeting of two different tumor markers in models of disseminated ovarian cancer. Two ovarian cancer cell lines (SKOV3 and SHIN3) were employed; both overexpress D-galactose receptor (D-galR), but only SKOV3 overexpresses HER2/neu. Additionally, fusion tumors composed of SKOV3 and SHIN3/RFP were evaluated. Both galactosyl serum albumin-rhodamine green (GSA-RhodG), which binds D-galR, and trastuzumab-Alexa680, which binds HER2/neu, were administered to tumor-bearing mice for *in vivo* fluorescence imaging and *in situ* fluorescence microscopy. *In vivo* fluorescence imaging depicted 64 of 69 SKOV3 tumors (94.2%) based on their dual spectra corresponding to both RhodG and Alexa680, while all 71 SHIN3 tumors (100%) were detected based on their single spectrum corresponding only to RhodG. All 59 SHIN3 and 36 SKOV3 tumors were correctly diagnosed with *in situ* microscopy. Additionally, in the mixed tumor model, all tumors could be depicted using the RhodG spectrum, but only SKOV3 components also showed the Alexa680 spectrum. In conclusion, multitargeted multicolor optical imaging enabled specific *in vivo* diagnosis of tumors expressing distinct patterns of receptors, leading to improved diagnostic accuracy. [DOI: 10.1117/1.3083449]

Keywords: molecular imaging; optical probe; cancer; multicolor; multitargeting.

Paper 08373R received Oct. 17, 2008; revised manuscript received Dec. 19, 2008; accepted for publication Dec. 23, 2008; published online Feb. 27, 2009.

1 Introduction

Optical imaging probes with targeting ligands directed at cell surface markers overexpressed on cancers have the potential to detect and characterize tumors *in vivo* with high sensitivity and specificity.[1–4] Such probes could help direct surgery[5] or guide nonconventional treatments, such as photodynamic therapy.[6] However, malignant tumors are notorious for their heterogenous and diverse expression of cell surface markers;[7] the degree and variety of target molecule expression may vary between and within tumor foci. Moreover, there is inevitably some low-level expression in normal tissue. However, by utilizing a strategy that employs more than one type of targeting ligand in a single imaging session, it should be possible to detect more tumor volume with great specificity than can be accomplished with a probe directed at a single target. Thus, if the simultaneous diagnosis of several targets on a tumor cell were possible *in vivo*, it could improve both tumor detection and characterization, potentially leading to more effective targeted therapy.

Herein, we describe the simultaneous use of two optical probes, each targeting a different cell surface marker and each conjugated to a different optical fluorophore. We employed two human ovarian cancer cell lines, SHIN3[8] and SKOV3,[9] which produce peritoneal dissemination when introduced into mice via intraperitoneal injection. Although both cell lines express D-galactose receptor (D-galR),[10] only SKOV3 also overexpresses HER2/neu.[9] We chose these receptor systems to demonstrate simultaneous multitarget molecular imaging because both of them are feasible for clinical application. D-galR is expressed by various ovarian cancer cells,[10] therefore, it is a good target for developing fluorescence-enhanced surgical guidance for disseminated peritoneal ovarian cancer. HER2/neu is a well-established cancer cell surface marker expressed on various cancers, including breast, colon, and ovarian. A humanized monoclonal antibody, trastuzumab, has been approved for a molecular-specific target cancer reagent by the FDA for patients with breast cancers that overexpress HER2/neu and is used commonly in clinical practice. We employed galactosyl serum albumin (GSA) conjugated Rhodamine Green (RhodG) to bind D-galR-expressing cells and trastuzumab conjugated Alexa680 to bind HER2/neu-expressing cells.[2,3] Given that SKOV3 expresses both targets, we predicted these cells would bind both GSA-RhodG and trastuzumab-Alexa680 while SHIN3 tumors, expressing only D-galR would only bind GSA-RhodG. Using this strategy we

Address all Correspondence to: Hisataka Kobayashi, M.D., Ph.D. Molecular Imaging Program, Center for Cancer Research, National Cancer Institute, NIH, Building 10, Room 1B40, MSC1088, Bethesda, MD 20892-1088. Tel: 301-451-4220; Fax: 301-402-3191; E-mail: kobayash@mail.nih.gov

1083-3668/2009/14(1)/014023/8/$25.00 © 2009 SPIE

demonstrate multiple targeting to a single tumor type and characterize the distribution of the surface marker expression *in vivo*.

2 Materials and Methods

2.1 *Cell Lines and Culture*

Two established human ovarian cancer cell lines (SKOV3 and SHIN3) were used in this study. SKOV3 overexpresses HER2/neu,[9] but both express D-galR.[10] SHIN3 cells were transfected with a plasmid expressing red fluorescent protein (RFP) to create a red fluorescent phenotype (SHIN3/RFP) that permitted optical identification of SHIN3-derived tumor implants, as previously described.[11] All cell lines were grown in RPMI 1640 medium (Invitrogen Corporation, Carlsbad, CA) containing 10% fetal bovine serum [(FBS), Invitrogen Corporation], 0.03% L-glutamine at 37 °C, 100 units/mL penicillin, and 100 μg/mL streptomycin in 5% CO_2.

2.2 *Synthesis of Rhodamine Green-Conjugated GSA*

GSA was purchased from Sigma Chemical (St. Louis, MO), amino-reactive Rhodamine Green (RhodG-NHS) was purchased from Invitrogen Corporation. At room temperature, 1 mg (13 nmol) of GSA in 0.1 M Na_2HPO_4 was incubated with 130 nmol of RhodG-NHS, at pH 8.5 for 30 min. The mixture was purified with a gel filtration column (Sephadex G50 column, PD-10; GE Healthcare, Piscataway, NJ) and the GSA binding fraction (2.7–4.5 mL) was eluted by 0.066 M PBS at pH 7.4 and collected in a test tube. GSA-RhodG was kept at 4 °C in the refrigerator as stock solutions. The protein concentrations of GSA-RhodG samples were determined with the Coomassie Plus protein assay kit (Pierce Biotechnology, Rockford, IL) by measuring the absorption at 595 nm with a ultraviolet-visible (UV-vis) system (8453 Value UV-Visible Value System, Agilent Technologies, Santa Clara, CA) using standard solutions of known concentrations of GSA (100 μg/mL). The concentration of RhodG was then measured by absorption at 503 nm with the UV-vis system to confirm the number of fluorophore molecules conjugated to each GSA molecule. The number of fluorophore molecules per GSA was adjusted to approximately 3–3.5.

2.3 *Synthesis of Rhodamine Green and Alexa680-Conjugated Trastuzumab*

Trastuzumab (Herceptin®), an FDA-approved humanized anti-HER2 antibody, which has a complimentary determination region against HER2 grafted on a human IgG1 framework, was purchased from Genentech Inc. (San Francisco, CA). RhodG-NHS and Alexa680-NHS were purchased from Invitrogen Corporation. At room temperature, 1 mg (6.8 nmol) of trastuzumab in 0.1 M Na_2HPO_4 was incubated with 68 nmol of RhodG-NHS or Alexa680-NHS, at pH 8.5 for 30 min. The mixture was purified with a gel filtration column (Sephadex G50 column, PD-10; GE Healthcare, Piscataway, NJ) and the antibody binding fraction (2.7–4.5 mL) was eluted by 0.066 M PBS at pH 7.4 and collected in a test tube. Trastuzumab-RhodG and trastuzumab-A680 were kept at 4 °C as stock solutions. The protein concentrations of samples were determined with the Coomassie Plus protein assay kit (Pierce Biotechnology, Rockford, IL) by measuring the absorption at 595 nm with a UV-vis system (8453 Value UV-Visible Value System, Agilent Technologies) using standard solutions of known concentrations of trastuzumab (200 μg/mL). The concentration of RhodG and Alexa680 was then measured by absorption at 503 and 679 nm, respectively, with the UV-vis system to confirm the number of fluorophore molecules conjugated to each trastuzumab molecule. The number of fluorophore molecules per trastuzumab was adjusted to approximately 3–3.5.

2.4 *In Vitro Fluorescence Microscopy*

Fluorescence microscopy was performed with an Olympus BX61 microscope (Olympus America, Inc., Melville, NY) equipped with the following filters: for the blue light filter, a bandpass filter from 470 to 490 nm and a bandpass filter from 515 to 550 nm were used for excitation and emission light, respectively; for the green light filter, the values were from 530 to 585 nm and from 605 to 680 nm, respectively, and for the red light filter, the values were from 590 to 650 nm and from 665 to 740 nm, respectively. Transmitted light differential interference contrast (DIC) images were also acquired.

Either SHIN3 cells (1×10^4) or SKOV3 cells (1×10^4) were plated on a cover glass–bottomed culture well and incubated at 37 °C in an atmosphere of 5% CO_2 for 16 h. GSA-RhodG (3 μg/mL), trastuzumab-Alexa680 (30 μg/mL), or both were added to the culture media. The cells were incubated and removed at the following time points: 1, 8, 24 h. Following removal, the cells were washed once with PBS, followed by fluorescence microscopy with the blue and red filter sets. To better localize the optical probes intracellularly, we also performed a colocalization study, adding 75 nM of the lysosomal marker (LysoTracker Red DND-99, Molecular Probe Inc., Eugene, OR) 1 h prior to imaging SKOV3 cells treated with either GSA-RhodG or trastuzumab-RhodG. LysoTracker selectively accumulates in the acidic compartments of the cell (i.e., the lysosome) and emits red fluorescence.[12] Fluorescence microscopy was performed with the blue, green, and red light filters at 1-h and 8-h time points.

To demonstrate dual targeting *in vitro*, a coculture of SKOV3 and SHIN3/RFP cells was created. Both SHIN3-RFP cells (1×10^4) and SKOV3 cells (1×10^4) were plated on a cover glass–bottomed culture well and incubated at 37 °C in a 5% CO_2 atmosphere for 16 h. Both GSA-RhodG (3 μg/mL) and trastuzumab-Alexa680 (30 μg/mL) were added to the culture media. The cells were incubated and removed at 1 and 8 h. Following removal, cells were washed once with PBS and fluorescence microscopy was immediately performed with the blue, green, and red light filters.

2.5 *Tumor Model*

All procedures were approved by the National Cancer Institute Animal Care and Use Committee. The tumor implants were established by intraperitoneal injection of 2×10^6 cells suspended in 200 μL of PBS in female nude mice (National Cancer Institute Animal Production Facility, Frederick, MD). Experiments with tumor-bearing mice were performed at 14 days for the SHIN3 mouse model and 35 days for the SKOV3 mouse model. Also, to establish a coincident tumor

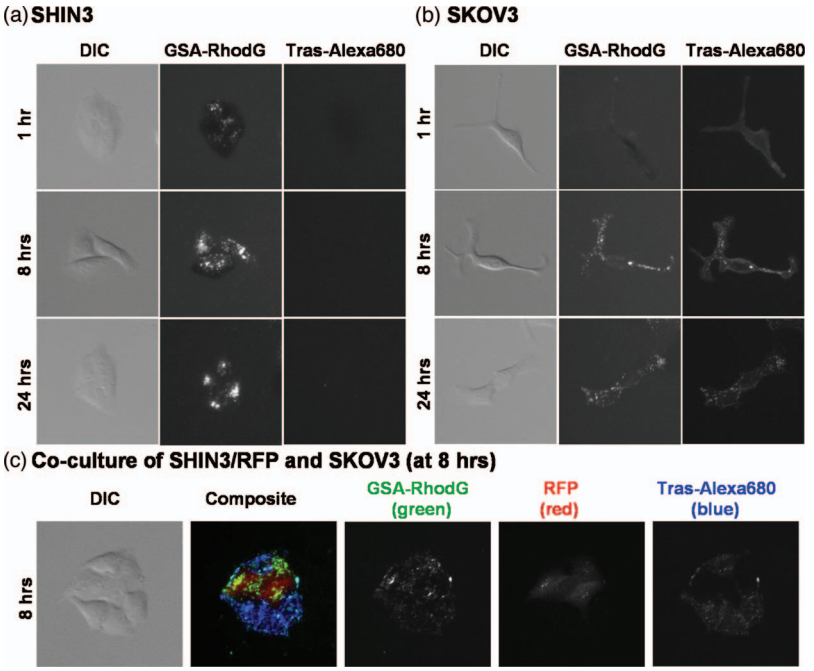

Fig. 1 Fluorescence microscopic images of SHIN3, SKOV3, and coculture of SHIN3/RFP and SKOV3 treated with the both GSA-RhodG 3 μg/mL and trastuzumab (Tras)-Alexa680 30 μg/mL. Camera exposure times were 200 ms for GSA-RhodG and 1 s for RFP and trastuzumab-Alexa680. (a) Fluorescence microscopic images of SHIN3 at 1 h shows binding of GSA-RhodG to SHIN3 cells as peripheral small fluorescent dots. After 8 h, the small dots spread homogenously throughout the cytoplasm and persisted at least 24 h. In contrast, trastuzumab-Alexa680 does not bind to SHIN3 cells at any time points. (b) SKOV3 cells show the binding of trastuzumab-Alexa680 to the HER2/neu receptor as rimlike fluorescence on the cell surface at 1 h. With time, the complexes are internalized into the cell and can be identified as small fluorescent dots at 8 h, which persist at least 24 h. Also, GSA-RhodG binds to SKOV3 cells with the similar binding pattern to SHIN3 cells. (c) In the coculture of SHIN3/RFP and SKOV3, SKOV3 cells are depicted by both GSA-RhodG and trastuzumab-Alexa680, while SHIN3/RFP cells are depicted by only GSA-RhodG. This reveals that *in vitro* dualtargeting of SKOV3 is feasible even when two cell lines are cocultured.

model, another group of mice received the intraperitoneal injection of SKOV3 cells (2×10^6 cells) followed seven days later by an intraperitoneal injection of SHIN3/RFP cells (2×10^6 cells). Experiments with SKOV3 and SHIN3/RFP tumor-bearing mice were performed at 30 days after injection of the SKOV3 cells.

2.6 *In Vivo Spectral Fluorescence Imaging*

After establishing the intraperitoneal dissemination model, groups of mice (four per group) with SHIN3, SKOV3, or the coincident model of SHIN3/RFP and SKOV3 were injected i.p. with 50 μg of trastuzumab-Alexa680 diluted with

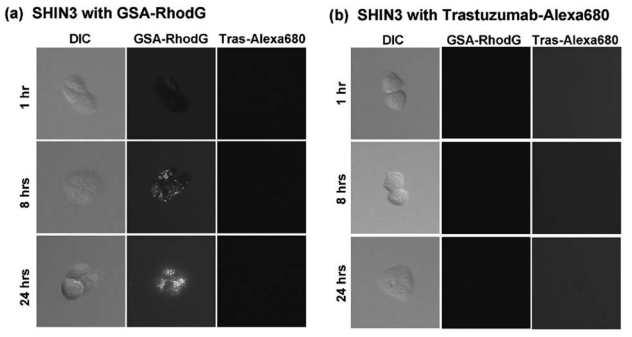

Fig. 2 Fluorescence microscopic images of SHIN3 treated with either GSA-RhodG (3 μg/mL) or trastuzumab (Tras)-Alexa680 (30 μg/mL). Exposure times were 200 ms for GSA-RhodG, and 1 s for trastuzumab-Alexa680. SHIN3 cells are depicted by GSA-RhodG, while are not depicted by trastuzumab-Alexa680. Binding patterns of GSA-RhodG are the same as those treated by the both GSA-RhodG and trastuzumab-Alexa680, as shown in Fig. 1(a).

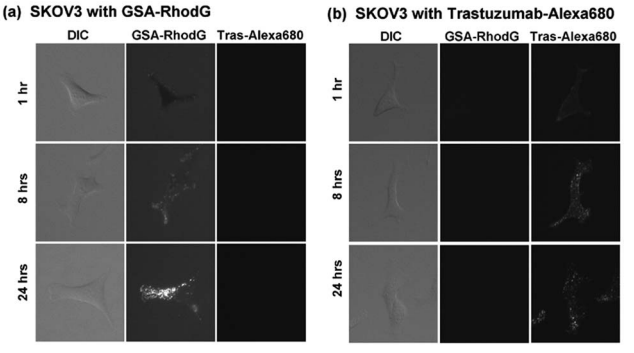

Fig. 3 Fluorescence microscopic images of SKOV3 treated with either GSA-RhodG (3 μg/mL) or trastuzumab (Tras)-Alexa680 (30 μg/mL). Camera exposure times were 200 ms for GSA-RhodG, and 1 s for trastuzumab-Alexa680. SKOV3 cells are depicted by the both GSA-RhodG and trastuzumab-Alexa680. Binding patterns of each probe are the same as those incubated with both GSA-RhodG and trastuzumab-Alexa680, as shown in Fig. 1(b).

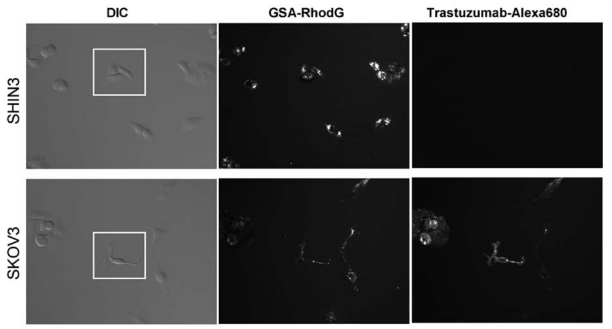

Fig. 4 In order to demonstrate the homogeneous targeting of cells with each reagent, low magnification microscopic images obtained 8 hrs after incubation are shown in comparison to the high magnification images shown in Fig. 1 (white squares in the DIC images).

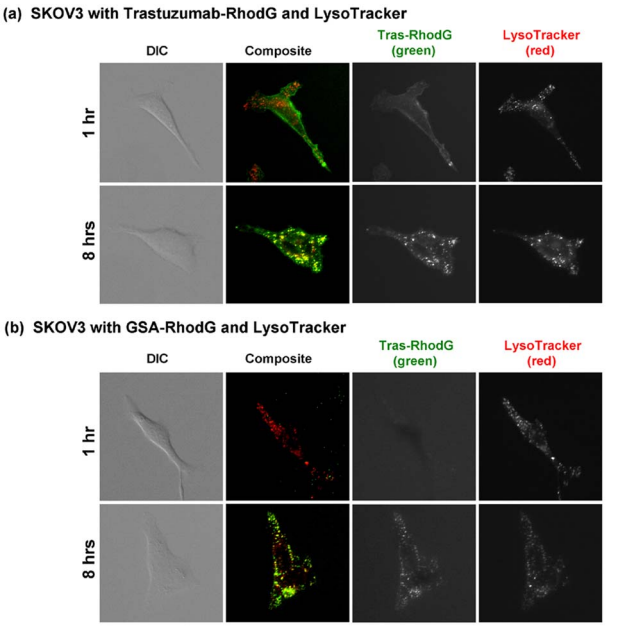

Fig. 6 Fluorescence microscopic images of SKOV3 treated with LysoTracker (75 nM) and either GSA-RhodG (3 μg/mL) or trastuzumab (Tras)-RhodG (3 μg/mL). Camera exposure times were 200 ms for GSA-RhodG, and 1 s for trastuzumab-RhodG and Lysotracker. (a) At 1 hr post incubation with trastuzumab-RhodG, trastuzumab-RhodG binds only to the cell surface, and does not co-localize to the lysosome as labeled by Lysotracker. However, at 8 hrs post incubation, Trastzumab-RhodG is internalized and distributed to the lysosomes which are identified as small dots co-localizing with Lysotracker. (b) With GSA-RhodG, small fluorescent dots can be identified at 8 hrs post incubation and correspond to the lysosome as labeled by Lysotracker. These small fluorescent dots were also identified at 1 hr, however, it was far less intense than those at 8 hrs, and not sufficient for co-localization study with LysoTracker.

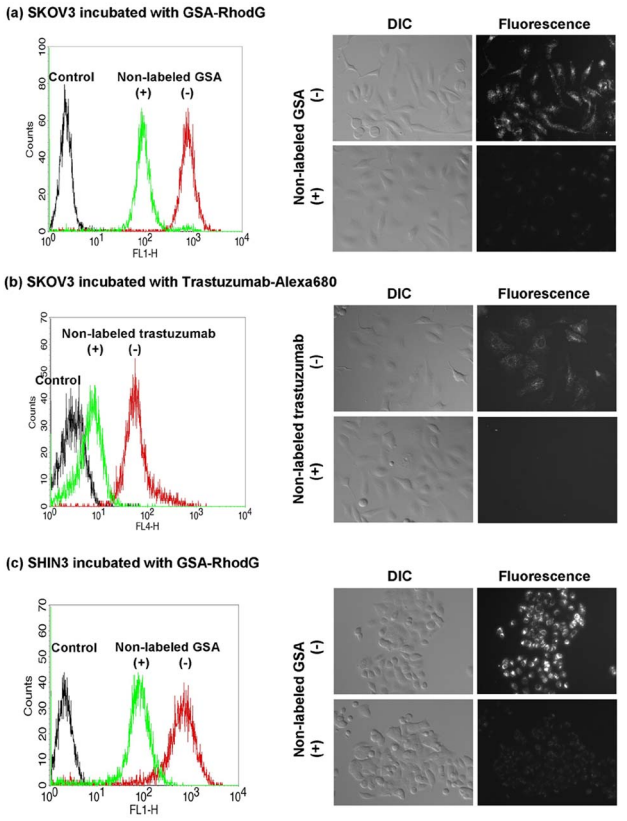

Fig. 5 In order to demonstrate the specific binding of each reagent, a blocking experiment was performed by adding 100-fold molar excess of non-labeled reagents 30 min prior to the start of incubation with each fluorescence-labeled reagents. The results were analyzed with both flow-cytometry and fluorescence microscopy. For both GSA and trastuzumab, the fluorescence signals from the target cells were significantly reduced by blocking with excess non-labeled reagents demonstrating that the binding of both GSA and trastuzumab to respective target cells was specific.

300 μL PBS, 24 h prior to imaging, followed by 25 μg of GSA-RhodG diluted with 300 μL PBS, 4 h prior to imaging. Mice were sacrificed with carbon dioxide, and then the abdominal cavities were exposed and the peritoneal membranes were spread on nonfluorescent black plates. Spectral fluorescence images were obtained using the Maestro *In Vivo* imaging system (CRi, Inc., Woburn, MA). Magnified multicolor spectral fluorescence images of the peritoneal membranes were obtained with a multiexcitation acquisition[13] using the blue-filter setting (excitation filter: 445–490 nm, emission filter: 515 nm long pass) and the red-filter setting (615–655 nm, 700 nm long pass) for the single-injected model, and the blue-filter, green-filter (503–555 nm, 580 nm long pass), and red-filter settings for the coincident tumor (SKOV3 and SHIN3/RFP) model. The tunable filter was automatically stepped in 10-nm increments from 500 to 800 nm for the blue-filter settings and from 650 to 950 nm for red-filter settings, while the camera sequentially captured images at each wavelength interval. The spectral fluorescence images consisting of autofluorescence spectra, RhodG, RFP, and Alexa680 were unmixed, using commercial software (Maestro software, CRi).

All spectral fluorescence images of tumor-bearing mice with a single tumor type underwent a region-of-interest

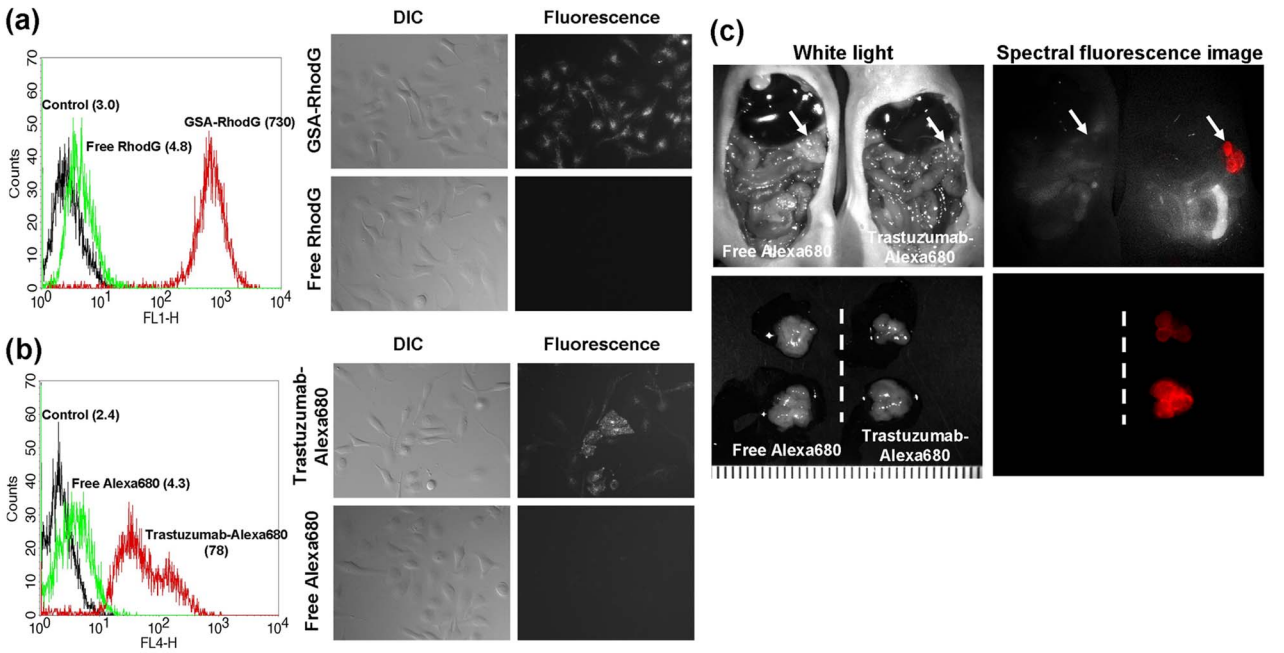

Fig. 7 In order to demonstrate that free dyes alone could not target cells, incubation studies with target cells were performed using same amount of targeted or free dyes. The results were analyzed with flow cytometry and fluorescence microscopy. Neither free RhodG (a) nor Alexa680 (b) dyes showed significant accumulation within SHIN3 (a) and SKOV3 (b) cells respectively. Moreover, free Alexa680 dyes did not show specific accumulation in the SKOV3 tumors in mice (c).

(ROI)–based analysis. First, all nodules, whose long axis was >0.5 mm, were identified on either unmixed RhodG or Alexa680 spectral images. Then, single maximum-sized ROIs were placed over those nodules using Image J software (http://rsbweb.nih.gov/ij/), and the average fluorescence intensity of each ROI was calculated. A "positive" nodule was defined as having an average fluorescence intensity of $\geqslant 25$ arbitrary units on unmixed images, whereas a "negative" nodule was defined as having an average fluorescence intensity of <25 arbitrary units. The number of positive nodules for both RhodG and Alexa680 and the number of positive nodules for either RhodG or Alexa680 were recorded.

2.7 *In Situ Fluorescence Microscopy*

After the surgical procedure described in the previous section, the abdominal contents were isolated and spread on a glass slide, and then subjected to *in situ* fluorescence microscopy using an Olympus BX61 microscope (Olympus America, Inc., Melville, NY). DIC imaging was used to guide spectral fluorescence imaging, which was performed either with a two-filter set for the single-tumor model or a three-filter set for the coincident tumor model. Only nodules sized from 0.5 to 2.5 mm on DIC images were included in this analysis.

3 Results

3.1 *In Vitro Fluorescent Microscopic Study*

Serial observations of SHIN3 and SKOV3 cells incubated with GSA-RhodG, trastuzumab-Alexa680, or the both were done using fluorescence microscopy (Fig. 1–4). Fluorescence microscopic images of SHIN3 cells demonstrated binding of GSA-RhodG to SHIN3 cells denoted by small, peripheral fluorescent dots within cells at 1 h postincubation [Fig. 1(a)]. After 8 h, the bright fluorescent dots had coalesced and remained present in the cytoplasm at the 24-h time point. Additionally, GSA-RhodG demonstrated a similar phenomenon when incubated with SKOV3 cells. Incubation of the two cell types individually with trastuzumab-Alexa680 failed to reveal binding of this probe to SHIN3 cell at any of the time points [Fig. 1(a)], whereas SKOV3 cells demonstrated cell-surface binding of trastuzumab-Alexa680 at 1 h [Fig. 1(b)]. The specific binding of each reagent was demonstrated with experiments with the similar setting but with blocking by addition of 100-fold excess nonlabeled reagent as shown in Fig. 5. At 8 h the probe was internalized, as evidenced by the presence of numerous intracellular fluorescent foci homogenously distributed in the cytoplasm, and remained present when imaged at the 24-h time point. These studies revealed that binding of GSA-RhodG to SKOV3 cells and SHIN3 cells was comparable while trastuzumab-Alexa680 bound only to SKOV3 cells. Additionally, even in the coculture model of SKOV3 and SHIN3/RFP cells, SKOV3 cells were depicted by both GSA-RhodG and trastuzumab-Alexa680, while SHIN3/RFP cells were depicted only by GSA-RhodG [Fig. 1(c)].

Fluorescence microscopy of SKOV3 cells exposed to either GSA-RhodG or trastuzumab-RhodG and incubated with Lysotracker was performed to localize the optical probes within the cell (Fig. 6). At 1 h postincubation, trastuzumab-RhodG bound only to the cell surface, and did not colocalize with the Lysotracker [Fig. 6(a)]. However, by 8 h postincubation, trastuzumab-RhodG had been internalized and could be identified as small dots, which colocalized to the lysosome. These results indicate that trastuzumab-RhodG binds to HER2/neu receptor expressed on the cell surface and then the

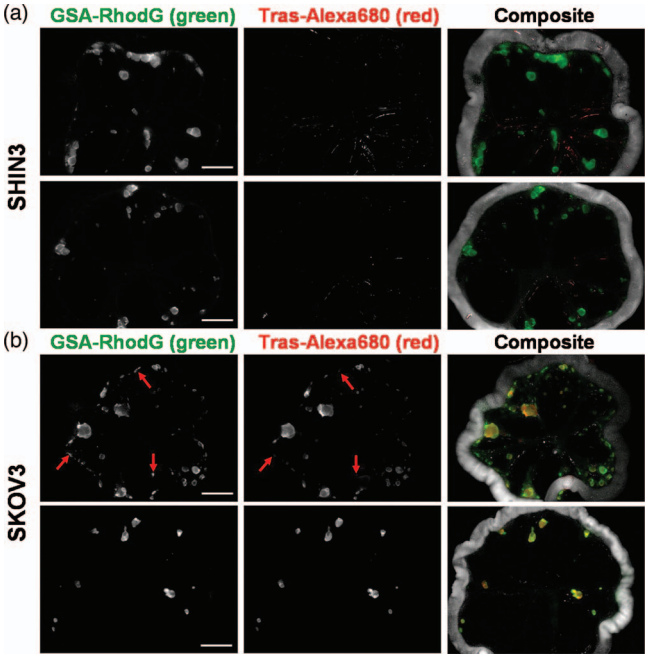

Fig. 8 *In vivo* multicolor spectral fluorescence images of single types of cells (either SHIN3 or SKOV3) exposed to both GSA-RhodG and trastuzumab (Tras)-Alexa680. White scale bars on GSA-RhodG spectral images indicate 5 mm. (a) In the SHIN3 group, the nodules depicted by GSA-RhodG spectral images do not appear on the trastuzumab-Alexa680 spectral images. (b) In the SKOV3 group, most of the nodules depicted on GSA-RhodG spectral images are also depicted on the trastuzumab-Alexa680 spectral images. However, in the upper images, the nodules depicted on GSA-RhodG spectral images are not shown on the trastuzumab-Alexa680 spectral images (arrows), resulting in examples of failure to label both targets of SKOV3.

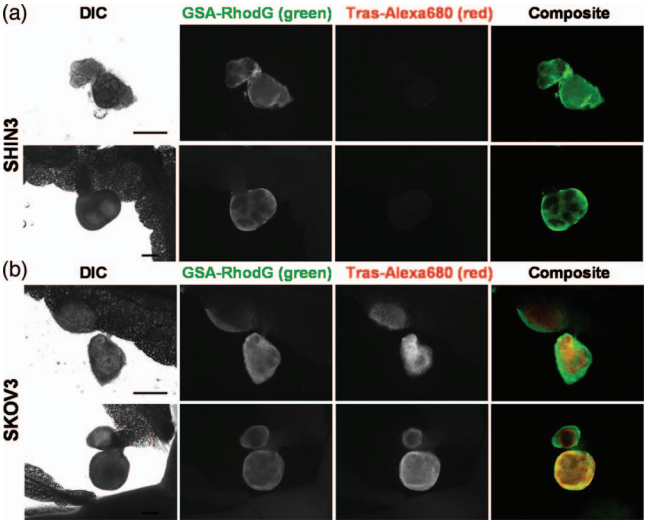

Fig. 9 *In situ* fluorescence microscopic images with single-injected tumor model of SHIN3 and SKOV3 treated with the both GSA-RhodG and trastuzumab (Tras)-Alexa680. Camera exposure times were 1 s for all fluorescence images. Black scale bars on DIC images indicate 0.5 mm. (a) Tumor nodules derived from SHIS3 cells are depicted by GSA-RhodG, while these are not depicted by trastuzumab-Alexa680. (b) Tumor nodules derived from SKOV3 cells are depicted by both GSA-RhodG and trastuzumab-Alexa680.

complex is internalized forming an endosome, later fusing with the lysosome to form an endolysosome structure. A similar phenomenon was seen with incubation with GSA-RhodG at 8 h postincubation, as small fluorescent dots were identified and corresponded to lysosomes labeled by Lysotracker [Fig. 6(b)].

3.2 *In Vivo Multicolor Spectral Fluorescence Imaging with Single-Tumor Model*

Seventy-one tumor nodules (>0.5 mm) could be identified on unmixed spectral images in four mice with SHIN3 tumors, while 69 tumor nodules (>0.5 mm) could be identified on unmixed spectral images in four mice with SKOV3 tumors. The mean size of the nodules was 1.23 ± 0.52 mm (mean ± sd) in the SHIN3 group, and 1.08 ± 0.56 mm in SKOV3 group. In the SHIN3 group, all 71 tumor nodules had emission spectra corresponding only to GSA-RhodG (71/71: 100%) and no tumor nodules had an emission spectra corresponding to trastuzumab-Alexa680 [Fig. 7 and 8(a)]. In the SKOV3 group, 64 nodules were successfully targeted with both targeting probes, visualized by the presence of a distinct spectra pattern comprised of both GSA-RhodG and Tratuzumab-Alexa680 spectra (64/69: 94.2%) [Fig. 8(b)]. However, five nodules failed to demonstrate the distinct emission spectra; three nodules were positive only for GSA-RhodG, while two nodules were positive only for tratuzumab-Alexa680.

3.3 *In Situ Fluorescence Microscopy Single-Tumor Model*

Fifty-nine tumor nodules (0.5–1.5 mm) could be identified on DIC images in four mice with SHIN3 tumors, while 36 tumor nodules (0.5–1.5 mm) could be identified on DIC images in four mice with SKOV3 tumors. Nodule size averaged 1.18 ± 0.47 mm (mean ± sd) in the SHIN3 group, and 0.98 ± 0.40 mm in the SKOV3 group. In the SHIN3 group, all 59 tumor nodules were depicted with GSA-RhodG and no signal corresponding to trastuzumab-Alexa680 was observed (59/59; 100%) [Fig. 9(a)]. In the SKOV3 group, all 36 nodules could be depicted with both GSA-RhodG and trastuzumab-Alexa680 (36/36; 100%) [Fig. 9(b)].

3.4 *In Vivo Multicolor Spectral Fluorescence Imaging and In Situ Fluorescence Microscopy in a Combined SKOV3 and SHIN3/RFP Tumor Model*

After establishing a reproducible mixed-tumor model composed of SKOV3 and SHIN3/RFP, we injected both GSA-RhodG and trastuzumab-Alexa680 into mixed-tumor–bearing mice to determine the capability of multiple targeting to distinguish SKOV3 containing tumors from SHIN3 containing tumors *in vivo* and in fusion tumors composed of both cell lines in the same animal. *In vivo* multicolor spectral fluorescence imaging showed that tumor nodules from SKOV3 lesions were easily identified by detection of Alexa680 and RhodG, but not the RFP spectrum that was the intrinsic marker for SHIN3 [Fig. 10(a)]. SHIN3/RFP lesions demonstrated RhodG and RFP spectra, but no Alexa680 spectrum.

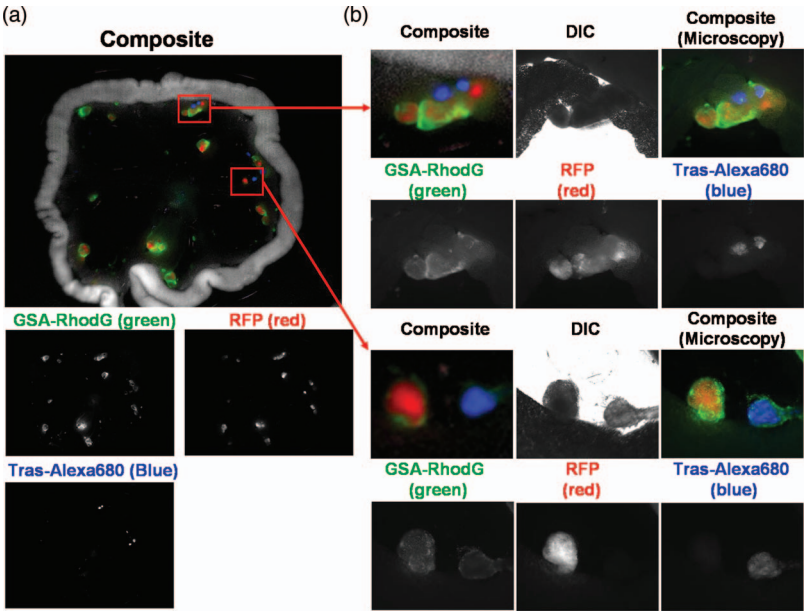

Fig. 10 *In vivo* multicolor spectral fluorescence images and *in situ* fluorescence microscopy with the coincident tumor model of SKOV3 and SHIN3/RFP exposed to both GSA-RhodG and trastuzumab (Tras)-Alexa680. Camera exposure times were 1 s for all fluorescence microscopic images. (a) *In vivo* multicolor spectral fluorescence images shows that all tumor nodules are depicted on GSA-RhodG spectral images, while only SKOV3 lesions, which do not have RFP labeling, are depicted on trastuzumab-Alexa680 spectral images. Thus, SKOV3 lesions are easily identified on the composite image even when they are mixed with other lesions. (b) *In situ* fluorescence microscopic images completely correspond to the result of *in vivo* multicolor spectral fluorescence images.

Furthermore, *in situ* fluorescence microscopy confirmed these results [Fig. 10(b)].

4 Discussion

In this study, we demonstrated the ability of two distinct optical probes, GSA-RhodG and trastuzumab-Alexa680, targeting different cell-surface markers, D-galR and HER2/neu, respectively, to distinguish two different cell lines of human ovarian cancer *in vivo*. Thus, SKOV3 cells, which express both D-galR and HER2/neu, can be distinguished from SHIN3 cells, which express only D-galR, even in tumor nodules that are composed of both cell types. Although such distinctions have been made *in vitro*, only recently has multitargeted *in vivo* imaging become feasible. This is made possible by multicolor spectral fluorescence imaging and fluorescence microscopy, which permit the spectral separation of RhodG and Alexa680 by using different excitation and emission filter sets as well as by using multiplexed targeted optical probes.

Muticolor fluorescence imaging has been performed mostly in the visible light range with fluorescent proteins.[14] With injectable fluorescent probes, a wider variety of wavelengths can be used for imaging. However, the only reason why Alexa680, a near-infrared fluorophore, was used was that it provided adequate spectral separation from RFP, which was the marker of SHIN3 cells. For surface applications, surgery assistance, or endoscopy, visible fluorescence is advantageous compared to near-infrared fluorescence. Because we used RFP as a validation tool, RhodG was a natural choice as an exogenous fluorophore because there was sufficient spectral separation between these two fluorophores. TAMRA, another desirable fluorophore,[15] has an emission spectra that overlaps with RFP. However, in clinical applications, where RFP is not present, the combination of TAMRA and RhodG might be ideal for dual targeting.

Although single target probes have demonstrated remarkably high specificity and sensitivity, false positives persist.[3] One advantage to using multiplexed targeted optical probes for tumor detection is that this approach reduces the number of false positives by increasing the specificity for tumor detection compared to a single-target-probe approach. Another advantage of this strategy is that it enables the detection and characterization of different types of tumor lesions, as shown in Fig. 10, in which all tumor nodules were detected by GSA-RhodG (a broadly sensitive probe), but only HER2/neu-expressing cells were detected with trastuzumab-Alexa680 (a highly specific probe). This strategy is akin to "*in vivo* immunohistochemistry" commonly used in modern pathology labs. Moreover, by changing the combination of targeted optical probes, it might be possible to distinguish a tumor lesion from surrounding inflammatory changes that are frequently found in clinical specimens (e.g., lung cancer associated with pneumonia), if probes specific for inflammatory markers were developed for optical imaging. Therefore, if combined with new technical advances in real-time fluorescence cameras,[5,16] a multiplex targeting approach could enable more detailed identification of tumors in real time and be useful during surgery or endoscopy.

In this study, there were five false negative nodules that were not detected with *in vivo* multicolor spectral fluorescence imaging. Although these tumor nodules yielded a signal, it was too weak and below the assigned cutoff value such that these tumors were not diagnosed correctly with the *in vivo* camera. It is likely that the delivery of the imaging agent

and/or excitation light to these tumors was insufficient due to the particular anatomic location or shape of these specific tumors. This problem would be less likely to occur during fluorescence microscopy because of the restricted and flat field of view and homogeneously strong lighting achievable with microscopy. With this in mind, it would be more likely to detect a lesion with fluorescence microscopy than with *in vivo* imaging, leading to false-negative results.

In conclusion, a method for *in vivo* simultaneous multitargeted optical imaging of different receptors was successfully established. This method may have implications for improving the diagnostic accuracy and therapeutic efficacy in cancer diagnosis and treatment.

Acknowledgment

This research was supported by the Intramural Research Program of the NIH, National Cancer Institute, Center for Cancer Research.

References

1. R. Weissleder and M. J. Pittet, "Imaging in the era of molecular oncology," *Nature (London)* **452**(7187), 580–589 (2008).
2. Y. Koyama, Y. Hama, Y. Urano, D. M. Nguyen, P. L. Choyke, and H. Kobayashi, "Spectral fluorescence molecular imaging of lung metastases targeting HER2/neu," *Clin. Cancer Res.* **13**(10), 2936–2945 (2007).
3. Y. Hama, Y. Urano, Y. Koyama, P. L. Choyke, and H. Kobayashi, "D-galactose receptor-targeted *in vivo* spectral fluorescence imaging of peritoneal metastasis using galactosamin-conjugated serum albumin-rhodamine green," *J. Biomed. Opt.* **12**(5), 051501 (2007).
4. J. V. Frangioni, "*In vivo* near-infrared fluorescence imaging," *Curr. Opin. Chem. Biol.* **7**(5), 626–634 (2003).
5. E. Tanaka, H. S. Choi, H. Fujii, M. G. Bawendi, and J. V. Frangioni, "Image-guided oncologic surgery using invisible light: completed pre-clinical development for sentinel lymph node mapping," *Ann. Surg. Oncol.* **13**(12), 1671–1681 (2006).
6. W. M. Sharman, J. E. van Lier, and C. M. Allen, "Targeted photodynamic therapy via receptor mediated delivery systems," *Adv. Drug Delivery Rev.* **56**(1), 53–76 (2004).
7. W. F. Anderson and R. Matsuno, "Breast cancer heterogeneity: a mixture of at least two main types?," *J. Natl. Cancer Inst.* **98**(14), 948–951 (2006).
8. S. Imai, Y. Kiyozuka, H. Maeda, T. Noda, and H. L. Hosick, "Establishment and characterization of a human ovarian serous cystadenocarcinoma cell line that produces the tumor markers CA-125 and tissue polypeptide antigen," *Oncology* **47**(2), 177–184 (1990).
9. M. C. Hung, X. Zhang, D. H. Yan, H. Z. Zhang, G. P. He, T. Q. Zhang, and D. R. Shi, "Aberrant expression of the c-erbB-2/neu protooncogene in ovarian cancer," *Cancer Lett.* **61**(2), 95–103 (1992).
10. A. J. Gunn, Y. Hama, Y. Koyama, E. C. Kohn, P. L. Choyke, and H. Kobayashi, "Targeted optical fluorescence imaging of human ovarian adenocarcinoma using a galactosyl serum albumin-conjugated fluorophore," *Cancer J. Sci. Am.* **98**(11), 1727–1733 (2007).
11. Y. Hama, Y. Urano, Y. Koyama, M. Kamiya, M. Bernardo, R. S. Paik, I. S. Shin, C. H. Paik, P. L. Choyke, and H. Kobayashi, "A target cell-specific activatable fluorescence probe for in vivo molecular imaging of cancer based on a self-quenched avidin-rhodamine conjugate," *Cancer Res.* **67**(6), 2791–2799 (2007).
12. L. E. Via, R. A. Fratti, M. McFalone, E. Pagan-Ramos, D. Deretic, and V. Deretic, "Effects of cytokines on mycobacterial phagosome maturation," *J. Cell. Sci.* **111**(7), 897–905 (1998).
13. Y. Koyama, T. Barrett, Y. Hama, G. Ravizzini, P. L. Choyke, and H. Kobayashi, "*In vivo* molecular imaging to diagnose and subtype tumors through receptor-targeted optically labeled monoclonal antibodies," *Neoplasia* **9**(12), 1021–1029 (2007).
14. M. Yang, P. Jiang, and R. M. Hoffman, "Whole-body subcellular multicolor imaging of tumor-host interaction and drug response in real time," *Cancer Res.* **67**(11), 5195–5200 (2007).
15. M. R. Longmire, M. Ogawa, Y. Hama, N. Kosaka, C. A. Regino, P. L. Choyke, and H. Kobayashi, "Determination of optimal rhodamine fluorophore for *in vivo* optical imaging," *Bioconjugate Chem.* **19**(8), 1735–1742 (2008).
16. M. Bouvet, J. Wang, S. R. Nardin, R. Nassirpour, M. Yang, E. Baranov, P. Jiang, A. R. Moossa, and R. M. Hoffman, "Real-time optical imaging of primary tumor growth and multiple metastatic events in a pancreatic cancer orthotopic model," *Cancer Res.* **62**(5), 1534–1540 (2002).